



Since January 2020 Elsevier has created a COVID-19 resource centre with free information in English and Mandarin on the novel coronavirus COVID-19. The COVID-19 resource centre is hosted on Elsevier Connect, the company's public news and information website.

Elsevier hereby grants permission to make all its COVID-19-related research that is available on the COVID-19 resource centre - including this research content - immediately available in PubMed Central and other publicly funded repositories, such as the WHO COVID database with rights for unrestricted research re-use and analyses in any form or by any means with acknowledgement of the original source. These permissions are granted for free by Elsevier for as long as the COVID-19 resource centre remains active.



Seawater fungi-derived compound screening to identify novel small molecules against dengue virus NS5 methyltransferase and NS2B/NS3 protease

Mahamudul Hasan^{b,*}, Md. Mukhtar Mia^{a,b,**}, Shahab Uddin Munna^{b,1},
Md. Mowdudul Hasan Talha^{b,c}, Kanon Das^{b,c}

^a Department of Poultry Science, Faculty of Veterinary, Animal and Biomedical Sciences, Sylhet Agricultural University, Sylhet, 3100, Bangladesh

^b Faculty of Veterinary, Animal and Biomedical Sciences, Sylhet Agricultural University, Sylhet, 3100, Bangladesh

^c Department of Pharmacology and Toxicology, Faculty of Veterinary, Animal and Biomedical Sciences, Sylhet Agricultural University, Sylhet, 3100, Bangladesh

ARTICLE INFO

Keywords:

Dengue virus
Marine-derived compounds
NS2B/NS3 protease
NS5 methyltransferase
Molecular docking
Target-prediction
Drug prediction

ABSTRACT

Dengue fever is a virus spread by mosquitoes that has no effective treatment or vaccination. Several dengue cases combined with the current COVID-19 pandemic, exacerbates this problem. Two proteins, NS5 methyltransferase and NS2B/NS3 primary protease complexes, are crucial for dengue viral replication and are the target sites for antiviral development. Thus, this study screened published literature and identified 162 marine fungus-derived compounds with active bioavailability. Following Lipinski's rules and antiviral property prediction, 41 compounds were selected for docking with NS5 methyltransferase and NS2B/NS3 protease (PDB ID: 6IZZ and 2FOM) to evaluate compounds that could stop the action of dengue viral protein complexes. To find the best candidates, computational ADME, toxicity, and drug target prediction were performed to estimate the potential of the multi-targeting fungal-derived natural compounds. Analyzing the result from 41 compounds, Chevalone E (−13.5 kcal/mol), Sterolic acid (−10.3 kcal/mol) showed higher binding energy against dengue NS2B/NS3 protease; meanwhile, Chevalone E (−12.0 kcal/mol), Brevione K (−7.4 kcal/mol), had greater binding affinity against NS5 methyltransferase. Consequently, this study suggests that Chevalone E is an effective inhibitor of NS5 methyltransferase and NS2B/NS3 protease. Ligand-based virtual screening from DrugBank was utilized to predict biologically active small compounds against dengue virus NS2B/NS3 major protease and NS5 methyltransferase. Both licensed medications, estramustine (DB01196) and quineprol (DB04575), were found to be similar to Chevalone E, with prediction scores of 0.818 and 0.856, respectively. In addition, cholic acid (DB02659), acitretin (DB00459), and mupirocin (DB00410) are similar to Sterolic acid, zidovudine (DB00495), imipenem (DB01598), and nadolol (DB01203) are similar to Brocazine A, and budesonide (DB01222) and colchicine (DB01394) are related to Brevione K. These findings suggest that these could be feasible dengue virus treatment options, meaning that more research is needed.

1. Introduction

Dengue virus (DENV) fever is the most common arthropod-borne viral disease in humans, affecting more than half of the world's population [1]. DENV of the Flaviviridae family is ubiquitous and has been reported in 953,476 cases in 2021 [2], the majority of which originated in Brazil, Peru, Vietnam, France, and the Philippines. Despite the

significant disease burden caused by DENV, there is no approved antiviral therapy or vaccine that can be used to treat or prevent infection [3]. The DENV genome is formed of 11 kb single-stranded positive sense RNA that is structured as 5'NCR-CprM-E-NS1-NS2A-NS2B-NS3-N-S4A-NS4B-NS5-3'NCR, where NCR is the noncoding region, C is the capsid, prM is the pre-membrane, E is the envelope, and NS is the nonstructural protein. Among these proteins, envelope glycoprotein,

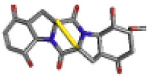
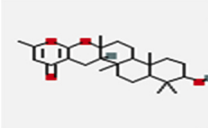
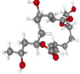
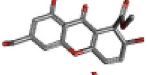
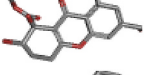
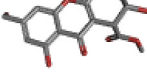
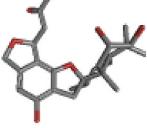
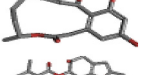
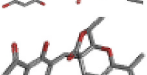

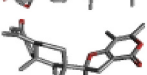
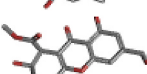
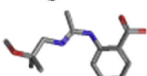
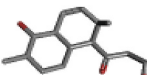
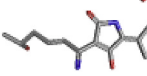
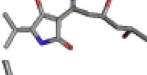
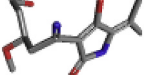
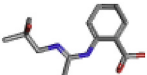

* Corresponding author.

** Corresponding author. Department of Poultry Science, Faculty of Veterinary, Animal and Biomedical Sciences, Sylhet Agricultural University, Sylhet, 3100, Bangladesh.

E-mail addresses: mhasan.student@sau.ac.bd (M. Hasan), mukhtar.psc@sau.ac.bd (Md.M. Mia).

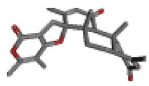
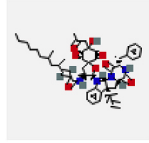
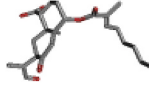
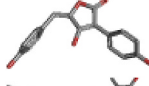
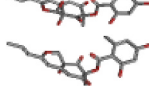
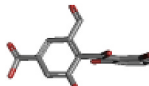
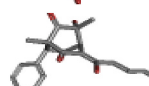
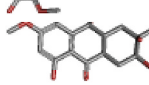
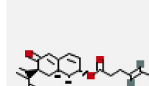

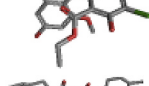
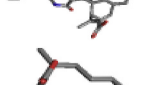
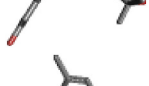
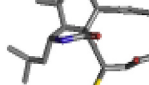
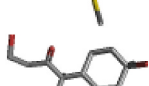
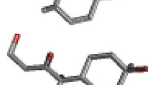
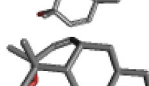
¹ Livestock Extension Officer, DLS, Bangladesh.

Table 1
List of selected bioactive compounds derived from sea water fungi with docked binding energy.

Compound Name	Compound Structure	Origin	2FOM	6IZZ	Reference
			Binding energy (kcal/mol)	Binding energy (kcal/mol)	
Brocazine A		<i>Penicillium brocae</i> MA-231	-8.6	-7.1	[39]
Chevalone E		<i>Aspergillus similanensis</i> sp.	-13.5	-12.0	[40]
Trichobotryside A		<i>Trichobotrys effuse</i> DFFSCS021	-7.5	-5.9	[41]
Engyodontiumone H		<i>Engyodontium album</i> DFFSCS021	-7.1	-5.8	[42]
Aspergillusone B		<i>Aspergillus sydowii</i> PSU-F154	-7.3	-6.3	[43]
Engyodontiumone F		<i>Engyodontium album</i> DFFSCS021	-6.9	-5.9	[42]
Stachybotrysin H		<i>Stachybotrys chartarum</i>	-8.3	-6.4	[44]
Dehydrocurvularin		<i>Penicillium</i> sp. SF-5859	-7.5	-6.3	[45]
Aspergifuranone		<i>Aspergillus</i> sp.	-8.3	-6.0	[46]
Penilactone A		<i>Penicillium crustosum</i>	-7.4	-6.1	[47]
Sterolic acid		<i>Penicillium</i> sp.	-10.3	-7.0	[48]
Brevione F		<i>Penicillium</i> sp.	-9.0	-7.1	[49]
Engyodontiumone C		<i>Engyodontium album</i> DFFSCS021	-7.5	-5.9	[42]
Penipacid B		<i>penicillium paneum</i>	-6.6	-5.7	[50]
Peaurantiogriseol A		<i>Penicillium aurantiogriseum</i> 328#	-6.3	-5.8	[51]
Cladosin C		<i>Cladosporium sphaerospermum</i> 2005-01-E3	-7.0	-5.9	[52]
Cladosin F		<i>Cladosporium sphaerospermum</i>	-6.7	-6.4	[52]
Cladosin G		<i>Cladosporium sphaerospermum</i>	-6.0	-5.8	[52]
Penipacid A		<i>penicillium paneum</i>	-6.9	-6.7	[50]

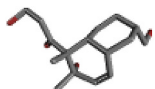
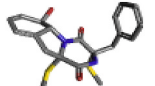
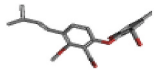

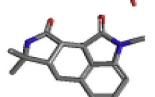
(continued on next page)

Table 1 (continued)

Compound Name	Compound Structure	Origin	2FOM	6IZZ	Reference
			Binding energy (kcal/mol)	Binding energy (kcal/mol)	
Brevione K		<i>Penicillium</i> sp.	-9.2	-7.4	[48]
Penicimutanin A		<i>Penicillium purpurogenum</i>	-7.6	-6.2	[53]
Integric acid		<i>Xylaria</i> sp.	-6.8	-5.3	[54]
Isoaspulvinone E		<i>Aspergillus terreus</i> Gwq-48	-8.1	-6.7	[55]
Purpurquinone B		<i>Penicillium funiculosum</i> No. 8974	-8.1	-6.4	[55]
Purpurquinone C		<i>Penicillium funiculosum</i> No. 8974	-7.8	-6.5	[56]
TAN-931		<i>Penicillium funiculosum</i> No. 8974	-7.4	-6.7	[57]
Sorbiccatechol A		<i>Penicillium chrysogenum</i> PJX-17	-8.1	-6.2	[58]
Tetrahydroaltersolanol C		<i>Alternaria</i> sp. ZJ-2008003	-8.6	-6.2	[59]
Acremeremophilane B		<i>Acremonium</i> sp.	-7.0	-5.6	[60]
Chrysine B		<i>Penicillium chrysogenum</i> SCSIO 41001	-6.6	-5.2	[61]
lindgomycin		Lingomycetaceae	-8.7	-6.8	[62]
Pseudaboydin A		<i>Pseudallescheria boydii</i>	-6.6	-6.5	[63]
Aspochalasin V		<i>Aspergillus</i> sp	-7.4	-5.7	[64]
Peaurantiogriseol C		<i>Penicillium aurantiogriseum</i> 328#	-6.4	-5.2	[51]
Peaurantiogriseol D		<i>Penicillium aurantiogriseum</i> 328#	-6.5	-5.2	[51]
Peaurantiogriseol E		<i>Penicillium aurantiogriseum</i> 328#	-7.0	-6.6	[51]

(continued on next page)

Table 1 (continued)

Compound Name	Compound Structure	Origin	2FOM	6IZZ	Reference
			Binding energy (kcal/mol)	Binding energy (kcal/mol)	
Peaurantiogriseol F		Penicillium aurantiogriseum 328#	-6.0	-5.0	[51]
Phomazine B		Phoma sp. OUCMDZ-1847vv	-7.3	-6.1	[65]
Penikellide A		Penicillium sp. MA-37	-7.5	-5.5	[66]
Resveratrodehyde A		Alternaria spp	-7.7	-6.5	[67]
Speradine G		Aspergillus oryzae	-7.7	-6.9	[68]

NS3 protease, NS3 helicase, NS5 methyltransferase, and NS5 RNA-dependent RNA polymerase have been proposed as potential therapeutic targets for dengue fever [4].

Antiviral research currently focuses on key viral enzymes associated with infection progression by inhibiting their biological activity directly or indirectly or by preventing the viral reproduction mechanism [5,6]. Several studies have revealed that NS2B/NS3 protease is one of the most commonly exploited targets for this purpose [7]. In addition, flavivirus

proteases, such as NS2B/NS3, are required to initiate viral replication with infectivity [4]. Furthermore, DENV infection is reduced by 80% when cells are treated with peptide inhibitors of these protease enzymes [8]. Presumably, in the case of therapeutic purpose, inhibiting viral proteases is a well-known method of avoiding viral infection. HIV protease inhibitors are widely used in clinical practice to treat HIV infection [9]. Similarly, simeprevir [10] and sofosbuvir [11] have recently been approved for therapeutic use against hepatitis C virus protease and have also been established as the gold standard. As a result, targeting NS2B/NS3 proteases with drugs is a widespread technique for treating DENV.

In recent years, marine fungi have been proven to be plentiful and a potential source of novel bioactive natural chemicals. Because most of these organisms exist in harsh environments, they can develop unique secondary metabolites. Metabolites are thought to represent the chemical defense response of fungi competing for substrates [12]. The range of natural chemicals produced by marine fungi suggests that some of these substances could be used in clinical trials to develop anti-infective medications.

Our study focused on using fungal bioactive compounds with potent antiviral activity against various known pathogenic viruses, such as influenza, hepatitis C virus, and herpes simplex virus, and as potential drug prototypes against DENV as a contribution to this global scientific endeavor. Thus, in this study, we used a systematic screening method to identify the top candidate for NS2B/NS3 and NS5 inhibitors of pathogenic DENV. Furthermore, computerized absorption, distribution, metabolism, excretion, and toxicity (ADMET) were analyzed to predict the potential of these multi-targeting fungal natural compounds for lead optimization and drug discovery.

2. Method and materials

2.1. Protein dataset and binding site analysis

X-ray crystallographic structures of nonstructural (NS) methyltransferase NS5 (PDB ID: 6IZZ) and NS2B/NS3 protease (PDB ID: 2FOM) were retrieved from the Protein Data Bank (PDB). Afterwards, active drug sites of two retrieved proteins were predicted using the Computed Atlas of Surface Topography of Proteins (CASTp) server for high-resolution crystal structures and binding pockets [13].

2.2. Protein and ligand preparation

Before docking investigations, each protein was opened into the

Table 2

H-bond interactions of top 5 potential compounds derived from marine fungi against dengue NS2b/NS3 protease and NS5 methyl transferase inhibitor.

2FOM	Fungi derived bioactive compound	Binding energy (kcal/mol)	Conventional Hydrogen bonding	Ligand binding amino acid with receptor
			Amino acid interaction: bond length (Å)	
2FOM	Chevalone E	-13.5	-	GLY153
	Sterolic acid	-10.3	SER127: 2.42, LEU128: 2.03, GLY153: 2.40, HIS51: 3.01	SER127, LEU128, ASP129, TYR161, GLY153, HIS51
	Brevione K	-9.2	ARG54: 1.76	LEU76, TRP83, ASP152
	Brevione F	-9.0	GLY153: 2.45	TYR161, LEU128, PRO132
	lindgomycin	-8.7	GLY151: 2.37	ASP75, GLY151, TYR161
61ZZ	Chevalone E	-12.0	-	LYS756, VAL785, TYR882
	Brevione K	-7.4	-	ASP808, THR806, MET809, TYR883, CYS780
	Brocazine A	-7.1	TYR838: 2.75, ILE717: 2.92	TYR838, GLY840, PRO837, ILE717
	Brevione F	7.1	-	PRO829, GLY819
	Sterolic acid	-7.0	ALA757: 2.26, TRP803: 3.16, GLU509: 3.04	GLU509, GLY510, TRP803, ALA757, TYR752

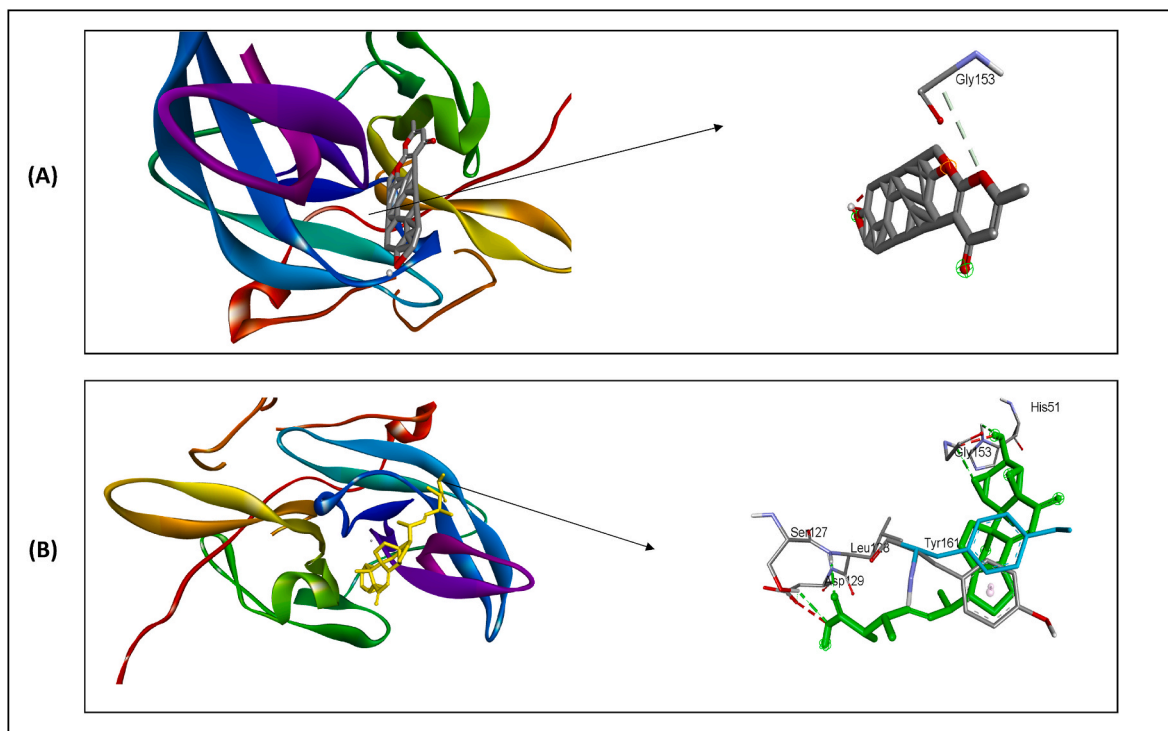


Fig. 1. Visualization of docked complex and ligand interaction with protein; (A) 2FOM-Chevalone E; (B) 2FOM-Sterolic Acid.

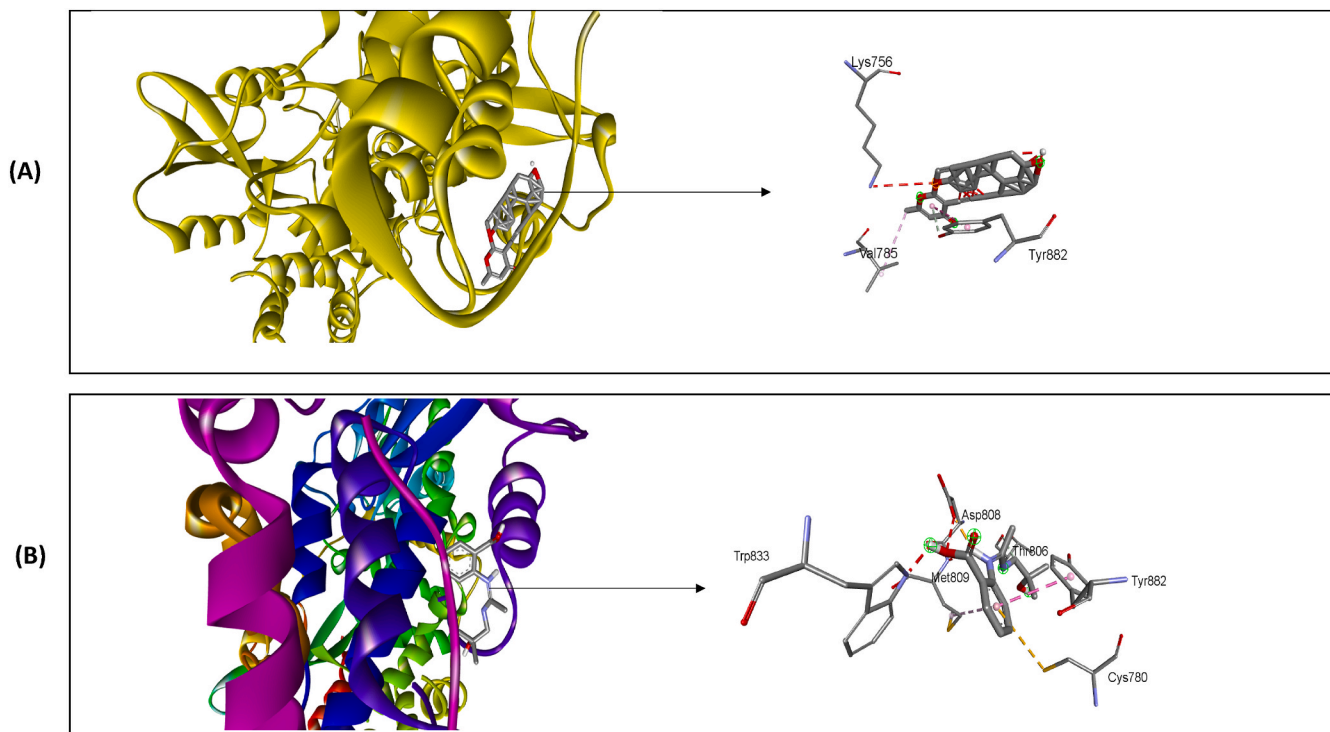


Fig. 2. Graphical presentation of docked complex and ligand interaction with protein; (A) 6IZZ-Chevalone E; (B) 6IZZ-Brevione K.

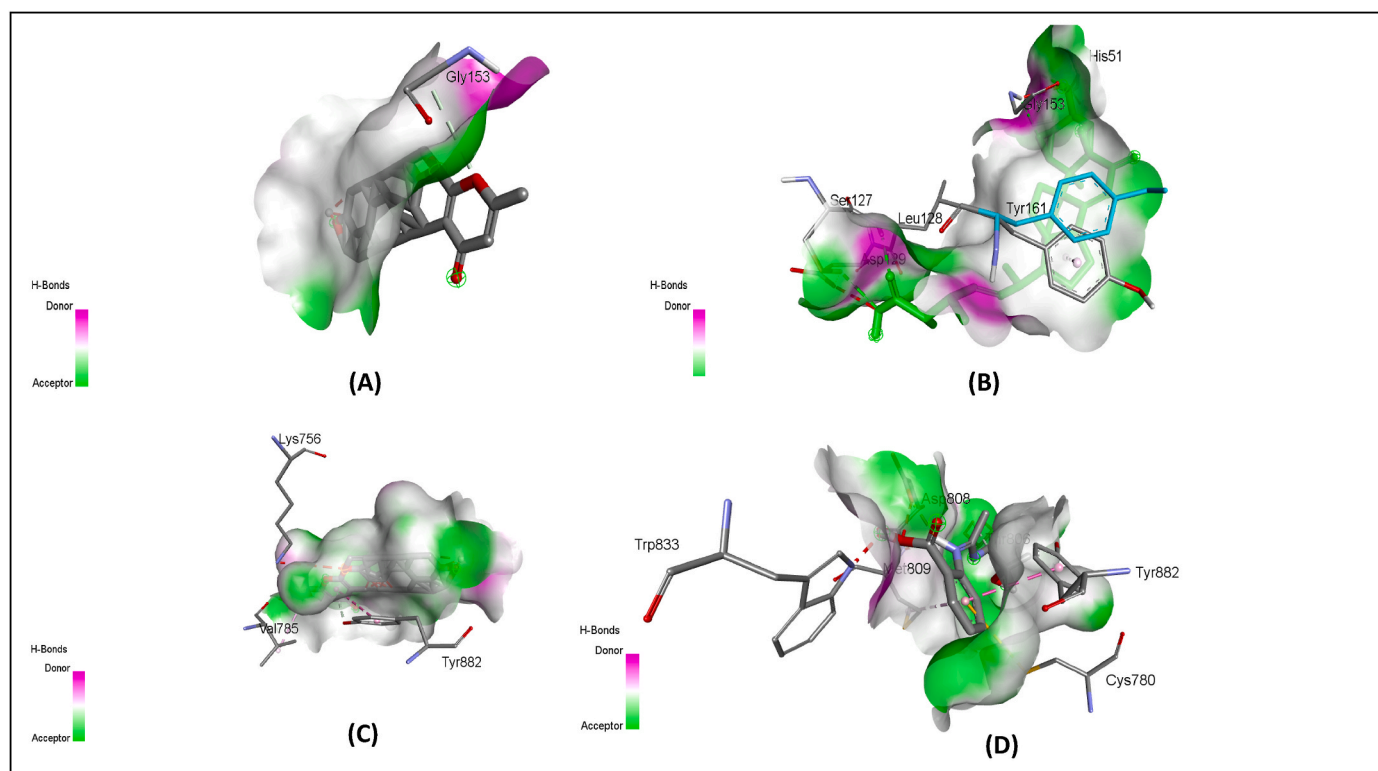


Fig. 3. Visualization of receptor-ligand hydrogen bond interaction(A) 2FOM-Chevalone E; (B) 2FOM-Sterolic Acid; (C) 6IZZ-Chevalone E; (D) 6IZZ-Brevione K.

Discovery Studio (DS) Visualizer, and water molecules, original inhibitor, and ligand compounds were removed to upgrade the protein's structure. The required hydrogen atoms were then inserted, followed by optimization to ensure structural stability. The final compounds were then translated to PDBQT format using the AutoDockTools-1.5.6 software.

To prepare the ligand, we examined a wide range of natural bioactive chemicals derived from marine fungi that have previously been outlined in the literature [14,15]. Subsequently, 162 compounds were enrolled with ID numbers and chemical structures obtained from the PubChem database (Supplementary Table 1). We then refined the bioactive compounds based on molecular weights between 350 and 500 (g/mol). Next, the biological potential of the selected compounds was predicted using the prediction service PassOnline server [16], which proposes the biological activity spectra of the compounds using the SMILES files of the structures. The likelihood of becoming active (pa) parameter was set to $pa > 0.3$ for a better prediction against DENV. Finally, 41 substances were found to have antiviral properties. Then, each ligand's SMILE file was converted to PDBQT format, loaded into the AutoDockTools-1.5.6 software, and set up using the prepared ligand preparation tool for docking analysis.

2.3. Active site prediction and molecular docking

For molecular docking experiments, we used the default procedure in

AutoDock tools 1.5.6 [17]. A grid box was created around the active site of DENV virus NS5 methyltransferase and NS2B/NS3 protease, as well as 2FOM and 6IZZ, with the help of a DS Visualizer. In addition, we set the grid box at $40 \times 40 \times 40$ points in the xyz-dimension, which equaled a grid box spacing of 0.3753, and fixed the coordinates of the x, y, and z centers as 0.387667, -6.969833, and 12.141667 for NS2B/NS3; meanwhile, -15.658143, -19.544214, and 38.773643 for NS5. We employed the Lamarckian genetic algorithm with default parameters for docking simulations, which included 10 genetic algorithm runs. Using the DS Visualizer, we further investigated the molecule with the highest energy ranking for protein-ligand interactions.

2.4. Drug profile analysis of top compounds

Absorption, distribution, metabolism, and excretion (ADME) are the four key criteria that determine drug levels and kinetics of drug exposure in an organism's tissues. These characteristics play a major role in the pharmacological activity and performance [18]. The SwissADME server was used to evaluate the ADME properties of the top five metabolites [19]. The blood-brain barrier (BBB) in the examined substances was calculated using the BOILED-Egg model [20].

2.5. Toxicity, carcinogenicity, and mutagenicity prediction

To predict toxicity, mutagenicity, and carcinogenic effects, canonical

Table 3
ADME properties of the best bioactive compounds derived from marine fungi.

	Compound	Chevalone E	Sterolic acid	Brevione K	Brocazine A	
Physicochemical Properties	Molecular weight	414.58	484.58	434.52	452.5	
	Num. heavy atoms	30	35	32	30	
	Num. atom. heavy atoms	6	0	6	0	
	Fraction Csp3	0.81	0.79	0.52	0.68	
	Num. rotatable bonds	0	5	0	1	
	Num. H-bond acceptors	4	7	5	7	
	Num. H-bond donors	1	2	1	2	
	Molar Refractivity	119.89	126.91	123.9	113.38	
	TPSA	59.67	108.89	73.58	175.05	
	Lipophilicity	Log Po/w (iLOGP)	4.1	3.05	3.58	1.51
Log Po/w (XLOGP3)		5.46	2.06	3.00	-2.16	
Log Po/w (WLOGP)		5.27	2.91	5.58	-1.69	
Log Po/w (MLOGP)		3.86	1.95	3.23	-1.61	
Log Po/w (SILICOS-IT)		5.42	4.09	3.53	-1.23	
Consensus Log Po/w		4.82	2.81	3.99	-1.04	
Log S (ESOL)		-6	-3.81	-4.56	-1.22	
Water Solubility	Solubility	4.16E-04	7.47E-02	1.19E-02	2.73E+01	
	Class	1.00E-06	1.54E-04	2.743-05	6.04E-02	
	Log S (Ali)	Moderately soluble	Soluble	Moderately soluble	Very soluble	
	Solubility	-6.47	-3.98	-4.21	-0.99	
	Class	1.40E-04	5.13E-02	2.68E-02	4.68E+01	
	Log S (SILICOS-IT)	3.39E-07	1.06E-04	6.17E-05	1.03E-01	
	Solubility	Poorly soluble	Soluble	Poorly soluble	Very soluble	
	Pharmacokinetics	GI absorption	High	High	High	Low
		BBB permeant	Yes	No	No	No
		P-gp substrate	No	Yes	No	Yes
CYP1A2 inhibitor		Yes	No	No	No	
CYP2C19 inhibitor		No	No	No	No	
CYP2C9 inhibitor		No	No	Yes	No	
CYP2D6 inhibitor		No	No	No	No	
CYP3A4 inhibitor		No	No	Yes	No	
Log Kp (skin permeation)		-4.95	-7.79	-6.87	-10.59	
Druglikeness		Lipinski	0	0	0	0
	Ghose	0	2	0	1	
	Veber	0	0	0	1	
	Egan	0	0	0	1	
	Muegge	1	0	0	2	
	Bioavailability Score	0.55	0.56	0.55	0.55	
	Medicinal Chemistry	PAINS	0	0	0	0
Brenk		0	2	0	1	
Leadlikeness		2	1	1	1	
Synthetic accessibility		5.96	7.41	6.17	6.16	

SMILES of the selected compounds that displayed predicted antiviral activity were uploaded to the pkCSM server [21] and proTox-II databases [22]. The toxicity was predicted using the toxicity mode in the pkCSM server, and the ProTox-II server was used to assess carcinogenicity and mutagenicity. By combining the molecular similarity, fragment tendency, and fragment similarity approaches, this popular server effectively predicts numerous toxicity outcomes [23]. Based on the analysis of 2-dimensional (2D) similarity to substances with a known median lethal dose, the server also projected the oral toxicity (LD50). The list used for the prediction contained almost 38,000 different chemicals with known oral LD50 values in mice [24].

2.6. Prediction of drug target and available drug molecules from DrugBank

The SwissTargetPrediction server was used to determine the potential macromolecular targets of the therapeutic candidates [25]. Based on a combination of 2D and 3D similarities with a library of 370,000 known bioactive chemicals on approximately 3000 proteins, the server makes predictions. Analyzing the homology screening of anticipated top drug candidates, the SwissSimilarity web tools were utilized to find possible therapeutic compounds against DENV virus NS5 methyltransferase and NS2B/NS3 protease. Using diverse methodologies, such as FP2 fingerprints, electroshapes, and spectrophores [26], the server allows ligand-based virtual screening of several libraries of small compounds to locate authorized, investigational, or commercially accessible

medications from DrugBank.

2.7. Molecular dynamics simulations

The iMOD server was used to analyze the structural dynamics of the best protein-ligand combination and to evaluate the stability of the structure by applying deformability analysis, which included the computation of the eigenvalues of the complexes [27,28]. This is a web server that can be customized and can generate complex deformability, variance, B-factor, covariance map data, and elastic network data. The deformability of a complex or protein is determined by its ability to deform at each amino acid residue [29]. The eigenvalue is equal to the energy difference required to bend a particular structure; therefore, the smaller the eigenvalue, the easier it is to deform the complex. The eigenvalue also represents the stiffness of the protein complex [30].

3. Results and discussion

3.1. Analysis of drug surface hotspot and ligand binding pocket

The drug surface hotspots of the selected NS5 methyltransferase and NS2B/NS3 protease with the ligand were investigated based on the structural conformation of the docked complexes. The ligand-binding patterns as well as the locations of the interacting residues are shown in Table 2. The positions of amino acids 127–161 were found to be crucial for NS2B/NS3 binding interactions (2FOM). Contrarily, the

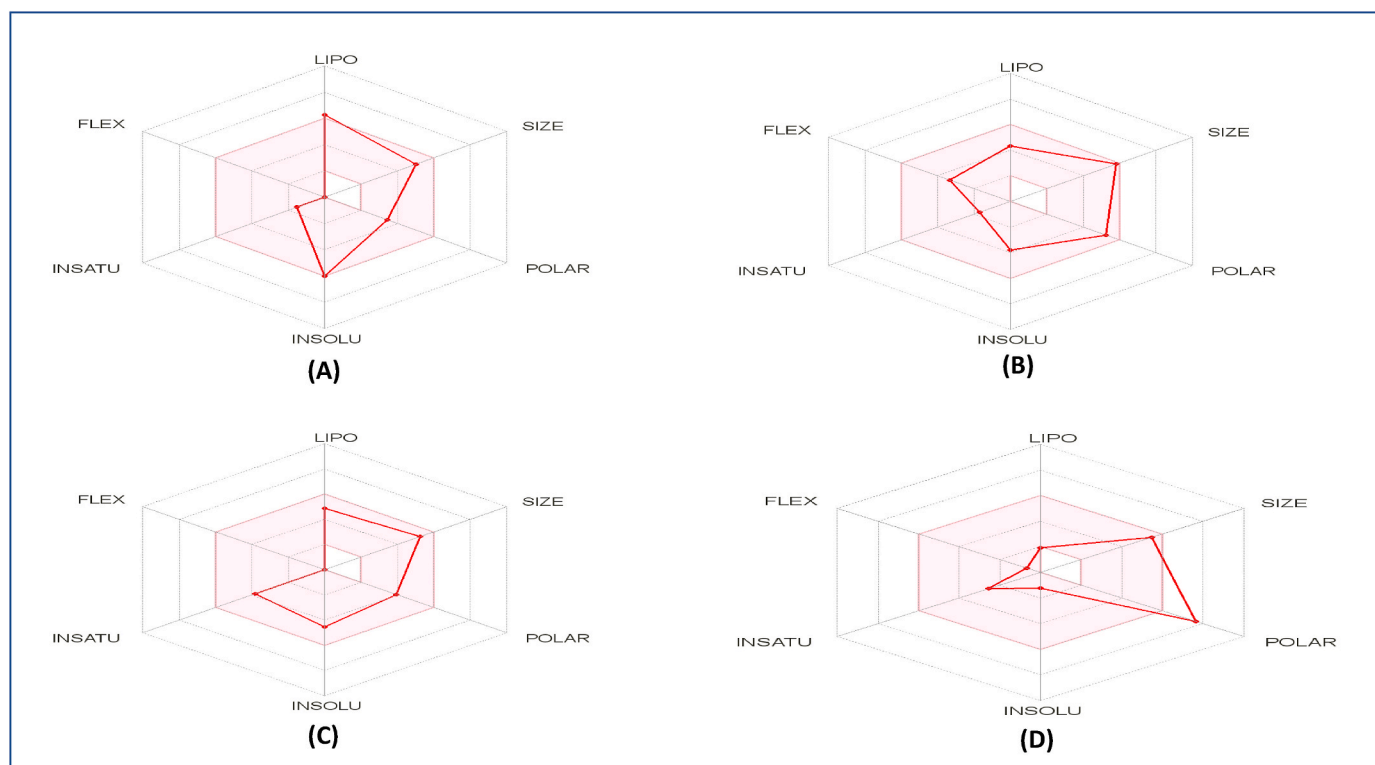


Fig. 4. ADME analysis of top four metabolites; (A) Chevalone E; (B) Sterolic Acid; (C) Brevione K; (D) Brocazine A.

amino acids from positions 806 to 840 showed the interactions with NS5 (6IZZ) protease. Additionally, CASTp was used to confirm the binding site residues of the two target proteins.

3.2. The binding affinities of the ligands into NS2B/NS3 and NS5 active site

The results of docking details were recovered after docking all the ligands with NS2B/NS3 protease and NS5 methyltransferase target in Table 1. The molecules that had the lowest binding energy of the docking score were considered the best molecules and had a higher binding affinity with the target receptors [31]. Moreover, the lower the stabilization energy of ligand binding to the receptor, the greater the potential of action was. To limit the probability of false-positive results, the ideal binding energy of marine fungal-derived compounds was compared with that of the approved clinical chemical treatments, and the binding energy in the screening criterion was amended to a negative value > -5 kcal/mol [32] to reduce the risk of false-positive results. The four best components are presented in Table 2, and the docking scores of all the compounds are listed in Table 1. Out of 41 compounds, including Chevalone E (-13.5 kcal/mol), Sterolic acid (-10.3 kcal/mol), Brevione K (-9.2 kcal/mol), Brevione F (-9.0 kcal/mol), lindgomycin (-8.7 kcal/mol), Tetrahydroaltersolanol C (-8.6 kcal/mol) showed higher binding energy against dengue NS2B/NS3 protease; meanwhile, Chevalone E (-12), Brevione K (-7.4 kcal/mol), Brocazine A (-7.1 kcal/mol), Brevione F (-7.1 kcal/mol), Sterolic acid (-7.0 kcal/mol), and Speradine G (-6.9 kcal/mol) had greater binding affinity against NS5

methyltransferase of dengue virus. Contrastingly, Peaurantiogriseols compounds, Penikellide A, Resveratroldehyde A, Remeremophilane B, and Engyodontiumone H showed the lowest binding affinity against viral NS5 methyltransferase but had moderate binding affinity against viral NS2B/NS3 protease.

In the previous study, the in-silico highest binding affinities of Artesunic acid and Homoeogonol against the NS5 methyl transferase reported as -7.2 and -7.1 kcal/mol [33], which refers the slightly higher binding affinity energy of our selected compounds (Chevalone E, Brevione K, Brocazine A, and Brevione F). In another study were revealed that apigenin and luteolin phytochemicals showed the highest binding affinity (-7.7 kcal/mol) against dengue NS2B/NS3 protease [34] that was dissimilar from our results we found more binding affinity -13.5 , -10.5 , -9.2 and -9.0 kcal/mol for Chevalone E, Sterolic acid, Brevione K, Brevione F, respectively. In addition, [35] reported a lower binding affinity for phytochemicals based on the binding affinity of the above-listed compounds. The ligand-receptor interactions are shown in Figs. 1 and 2.

3.3. Hydrogen bond analysis

The complex interactions between NS2B/NS3 and NS5 with inhibitory ligands were visualized using a DS Visualizer, and a hydrogen bond analysis was also performed. In the Table 2, the numbers of hydrogen bonds and residues implicated in hydrogen bond interactions were summarized. Chevalone E, Sterolic acid, Brocazine K, Brevione F, and lindgomycin are possible NS2B/NS3 inhibitor candidates with drug-like

Table 4
Toxicogenicity, mutagenicity and carcinogenicity prediction of selected bioactive compounds.

Bioactive compounds name	Chevalone E	Sterolic Acid	Brevione F	Brocazine A
AMES toxicity	No	No	No	No
hERG I inhibitor	No	No	No	No
hERGII inhibitor	No	No	No	No
Oral Rat Acute Toxicity (LD50)	2.122	2.541	2.664	3.486
Oral Rat Chronic Toxicity (LOAEL)	0.891	1.437	1.477	1.983
Hepatotoxicity	No	No	No	No
Skin Sensitisation	No	No	No	No
Minnow toxicity	1.015	0.973	0.25	5.734
Mutagenicity	Inactive (0.82)	Inactive (0.80)	Inactive (0.84)	Inactive (0.69)
Carcinogenicity	Inactive (0.67)	Inactive (0.54)	Inactive (0.53)	Inactive (0.69)
Immunotoxicity	Active (0.90)	Active (0.97)	Active (0.99)	Active (0.64)
Aryl hydrocarbon Receptor (AhR)	Inactive (0.96)	Inactive (0.92)	Inactive (0.92)	Inactive (0.92)
Androgen Receptor (AR)	Inactive (0.88)	Inactive (0.60)	Inactive (0.63)	Inactive (0.94)
Androgen Receptor Ligand Binding Domain (AR-LBD)	Inactive (0.86)	Inactive (0.53)	Inactive (0.52)	Inactive (0.94)
Aromatase	Inactive (0.76)	Inactive (0.58)	Inactive (0.58)	Inactive (0.90)
Estrogen Receptor Alpha (ER)	Inactive (0.72)	Inactive (0.65)	Inactive (0.65)	Inactive (0.88)
Estrogen Receptor Ligand Binding Domain (ER-LBD)	Inactive (0.90)	Inactive (0.90)	Inactive (0.89)	Inactive (0.92)
Peroxisome Proliferator Activated Receptor Gamma (PPAR-Gamma)	Inactive (0.85)	Inactive (0.85)	Inactive (0.84)	Inactive (0.89)
Nuclear factor (erythroid-derived 2)-like 2/antioxidant responsive element (nrf2/ARE)	Inactive (0.83)	Inactive (0.93)	Inactive (0.90)	Inactive (0.87)
Heat shock factor response element (HSE)	Inactive (0.83)	Inactive (0.93)	Inactive (0.90)	Inactive (0.87)
Mitochondrial Membrane Potential (MMP)	Inactive (0.56)	Inactive (0.62)	Inactive (0.52)	Inactive (0.83)
Phosphoprotein (Tumor Suppressor) p53	Inactive (0.72)	Inactive (0.58)	Inactive (0.57)	Inactive (0.84)
ATPase family AAA domain-containing protein 5 (ATAD5)	Inactive (0.95)	Inactive (0.91)	Inactive (0.92)	Inactive (0.92)

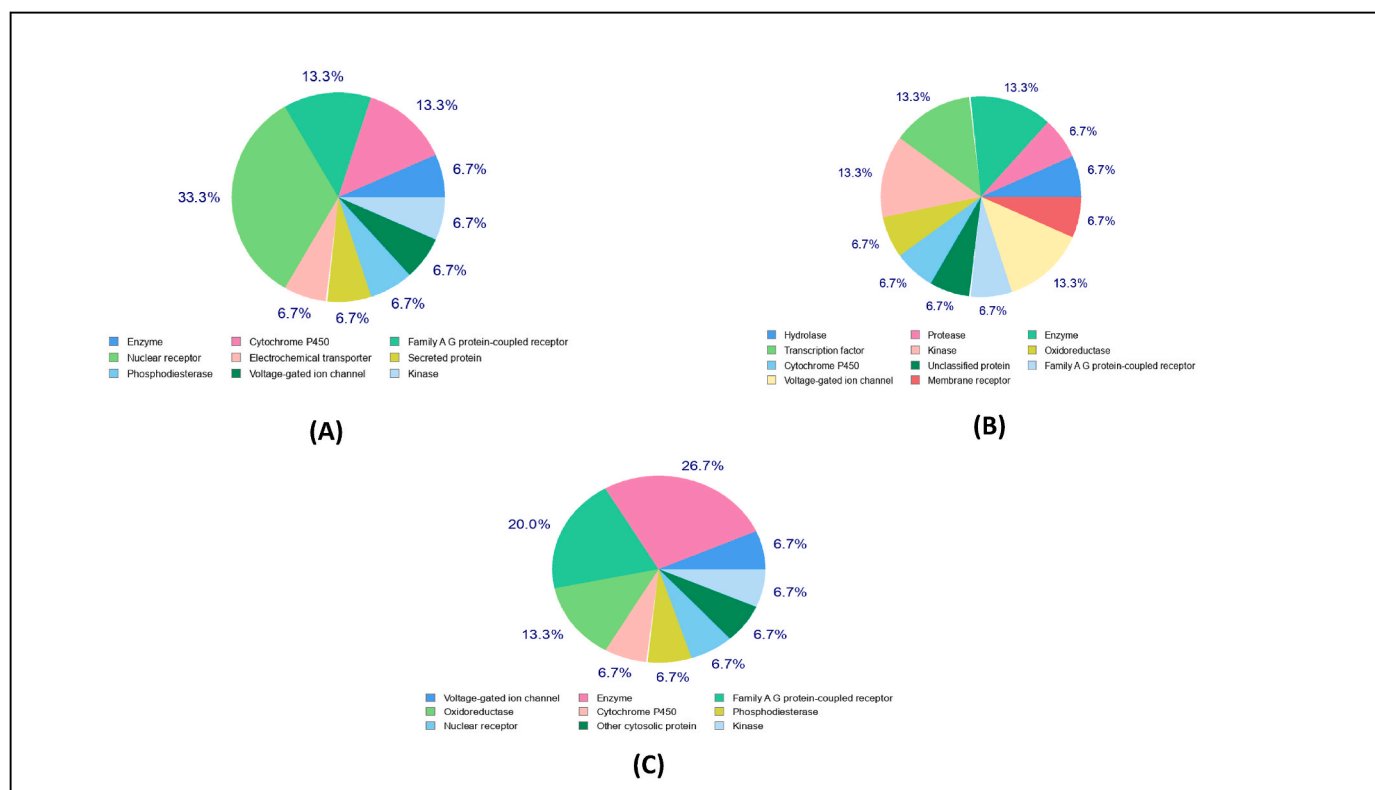


Fig. 5. Prediction of drug targets for (A) Chevalone E (B) Sterolic Acid, and (C) Brevione K.

properties and no toxicity, carcinogenicity, or mutagenicity. At the residues of SER127, LEU128, GLY153, and HIS51, Sterolic acid forms four hydrogen bonds, whereas only the ARG54 residue was formed in the case of Brocazine K. Moreover, Brevione F and Lindgomycin (GLY151: 2.37) showed that they could also be used as NS2B/NS3 inhibitors. Contrarily, at the residues TYR838 and ILE717, Brocazine A formed hydrogen bonds with viral NS5 methyltransferase. In addition, Sterolic acid had three hydrogen bonds interacting with the active site of NS5 methyltransferase at residues ALA757, TRP803, and GLU509.

Interestingly, despite the fact that Brevione K had a higher binding affinity, this combination was unable to form hydrogen bonds. Therefore, Brocazine A, with two hydrogen bonds, was found to be the best inhibitor of NS5 methyltransferase. The common interactions of the examined compounds, when compared to the original inhibitor, suggest that marine-derived fungal compounds Chevalone E, Sterolic acid, Brevione K, and Brocazine A (Fig. 3) could be potential inhibitors of NS2B/NS3 protease and NS5 methyltransferase.

Table 5
Predicted drug targets for Sterolic Acid, Brevione K, and Chevalone E.

	Target	Common name	UniProtKB ID	Target Class	Probability
Sterolic Acid	Sarcoplasmic/endoplasmic reticulum calcium ATPase 1	ATP2A1	O14983	Hydrolase	0.1106122
	Subtilisin/kexin type 7	PCSK7	Q16549	Protease	0.1106122
	Isoleucyl-tRNA synthetase	IARS	P41252	Enzyme	0.1106122
	Proto-oncogene c-JUN	JUN	P05412	Transcription factor	0.1106122
	Protein kinase C alpha	PRKCA	P17252	Kinase	0.1106122
	Cyclooxygenase-2	PTGS2	P35354	Oxidoreductase	0.1106122
	Glutathione S-transferase Mu 1	GSTM1	P09488	Enzyme	0.1106122
	Protein kinase C epsilon	PRKCE	Q02156	Kinase	0.1106122
	Cytochrome P450 19A1	CYP19A1	P11511	Cytochrome P450	0.1106122
	LanC-like protein 2	LANCL2	Q9NS86	Unclassified protein	0.1106122
	Proteinase-activated receptor 2	F2RL1	P55085	Family A G protein-coupled receptor	0.1106122
	Voltage-gated potassium channel subunit Kv1.3	KCNA3	P22001	Voltage-gated ion channel	0.1106122
	Transient receptor potential cation channel subfamily V member 4 (by homology)	TRPV4	Q9HBA0	Voltage-gated ion channel	0.1106122
	Integrin alpha-4/beta-1	ITGB1 ITGA4	P05556	Membrane receptor	0.1106122
Brevione K	Zinc finger protein GLI1	GLI1	P08151	Transcription factor	0.1106122
	Voltage-gated potassium channel subunit Kv1.5	KCNA5	P22460	Voltage-gated ion channel	0.106542926
	Protein farnesyltransferase	FNTA FNTB	P49354	Enzyme	0.106542926
			P49356		
	11-beta-hydroxysteroid dehydrogenase 1	HSD11B1	P28845	Enzyme	0.106542926
	C-C chemokine receptor type 5	CCR5	P51681	Family A G protein-coupled receptor	0.106542926
	Steroid 5-alpha-reductase 1	SRD5A1	P18405	Oxidoreductase	0.106542926
	Steroid 5-alpha-reductase 2	SRD5A2	P31213	Oxidoreductase	0.106542926
	Cytochrome P450 19A1	CYP19A1	P11511	Cytochrome P450	0.106542926
	Phosphodiesterase 10A (by homology)	PDE10A	Q9Y233	Phosphodiesterase	0.106542926
	Telomerase reverse transcriptase	TERT	O14746	Enzyme	0.106542926
	Orexin receptor 2	HCRTR2	O43614	Family A G protein-coupled receptor	0.106542926
	Orexin receptor 1	HCRTR1	O43613	Family A G protein-coupled receptor	0.106542926
	Glucocorticoid receptor	NR3C1	P04150	Nuclear receptor	0.106542926
Kinesin-like protein 1	KIF11	P52732	Other cytosolic protein	0.106542926	
PI3-kinase p110-alpha subunit	PIK3CA	P42336	Enzyme	0.106542926	
MAP kinase p38 alpha	MAPK14	Q16539	Kinase	0.106542926	
Chevalone E	11-beta-hydroxysteroid dehydrogenase 1	HSD11B1	P28845	Enzyme	0.106165761
	Cytochrome P450 17A1	CYP17A1	P05093	Cytochrome P450	0.106165761
	Serotonin 2b (5-HT2b) receptor	HTR2B	P41595	Family A G protein-coupled receptor	0.106165761
	Androgen Receptor (by homology)	AR	P10275	Nuclear receptor	0.106165761
	Adrenergic receptor alpha-2	ADRA2C	P18825	Family A G protein-coupled receptor	0.106165761
	Glucocorticoid receptor	NR3C1	P04150	Nuclear receptor	0.106165761
	Estrogen receptor alpha	ESR1	P03372	Nuclear receptor	0.106165761
	Serotonin transporter	SLC6A4	P31645	Electrochemical transporter	0.106165761
	Testis-specific androgen-binding protein	SHBG	P04278	Secreted protein	0.106165761
	Cytochrome P450 19A1	CYP19A1	P11511	Cytochrome P450	0.106165761
	Phosphodiesterase 10A	PDE10A	Q9Y233	Phosphodiesterase	0.106165761
	Voltage-gated potassium channel subunit Kv1.3	KCNA3	P22001	Voltage-gated ion channel	0.106165761
	Estrogen receptor beta	ESR2	Q92731	Nuclear receptor	0.106165761
	Peroxisome proliferator-activated receptor gamma	PPARG	P37231	Nuclear receptor	0.106165761
Tyrosine-protein kinase FYN	FYN	P06241	Kinase	0.106165761	

Table 6
Predicted drug targets for Chevalone E, Sterolic acid, Brevione K, and Brocazine A.

Metabolites	Screening method	Drug bank id	Name	Score	Status
Chevalone E	Electroshape	DB01196	Estramustine	0.818	Approved
	Spectrophores	DB04575	Quinestrol	0.856	Approved
Sterolic acid	FP2	DB00410	Mupirocin	0.73	Approved
	Electroshape	DB02659	Cholic Acid	0.89	Approved
Brevione K	Spectrophores	DB00459	Acitretin	0.84	Approved
	Electroshape	DB01394	Colchicine	0.85	Approved
Brocazine A	Spectrophores	DB01222	Budesonide	0.89	Approved
	FP2	DB00495	Zidovudine	0.865	Approved
A	Electroshape	DB01203	Nadolol	0.864	Approved
	Spectrophores	DB01598	Imipenem	0.860	Approved

3.4. In silico evaluation of drug likeness and ADME

The ADME approach was used to analyze the drug-likeness of the top four compounds found in the marine-derived fungi. Forecasts were made using the SwissADME database. The likeness of the drug was demonstrated by five rules established by Lipinski. The molecular weight (MW) should be between 350 and 500 (g/mol), the number of hydrogen bond acceptors should be between (10), the number of hydrogen bond donors should be between (5), and the Log Po/w should be between 5 and 10 [36], with no more than one violation allowed. Chevalone E, Brevione K, and Sterolic acid had higher gastrointestinal absorption than Brocazine A. Furthermore, the BOILED-Egg model was used to compute BBB penetration, which demonstrated that none of the top medication candidates tested had BBB permeation. Each compound was water soluble to varying degrees, with Sterolic acid having the

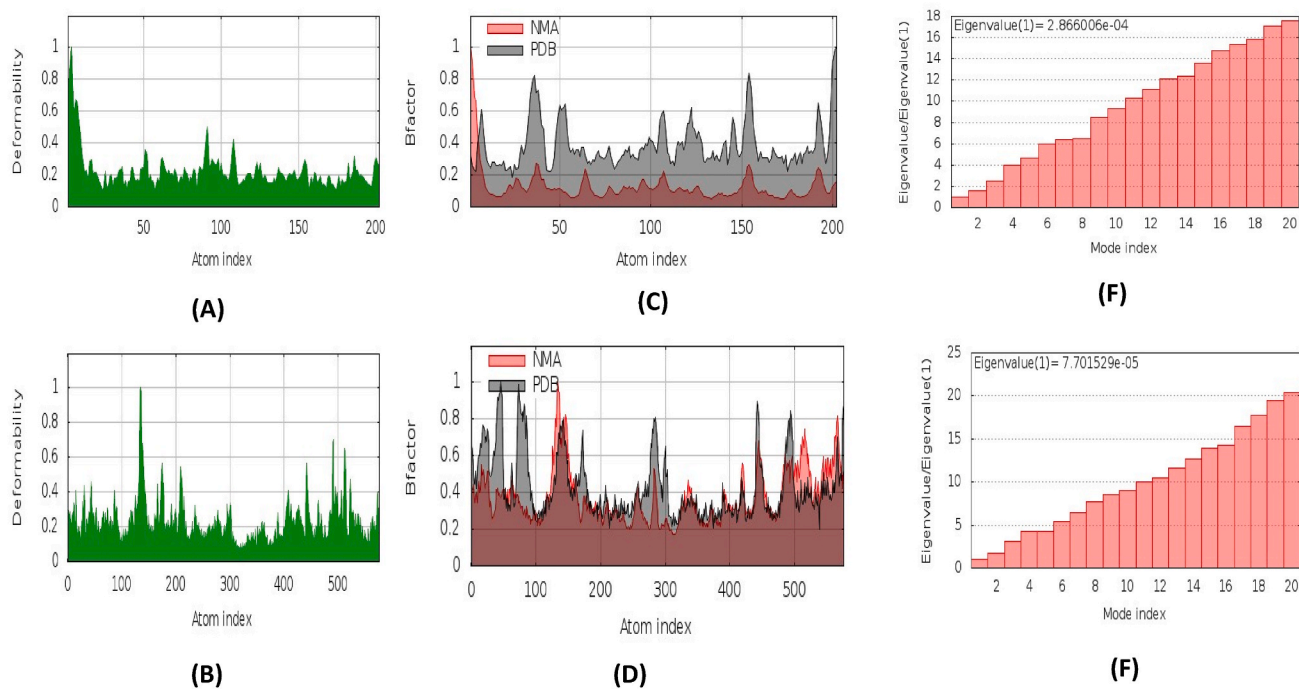


Fig. 6. Molecular dynamics simulation analysis, deformability: (A) Chevalone E – NS2B/NS3 protease, (B) Chevalone E – NS5 methyltransferase; Bfactor: (C) Chevalone E – NS2B/NS3 protease, (D) Chevalone E – NS5 methyltransferase; and stability (eigen value): (E) Chevalone E – NS2B/NS3 protease, (F) Chevalone E – NS5 methyltransferase.

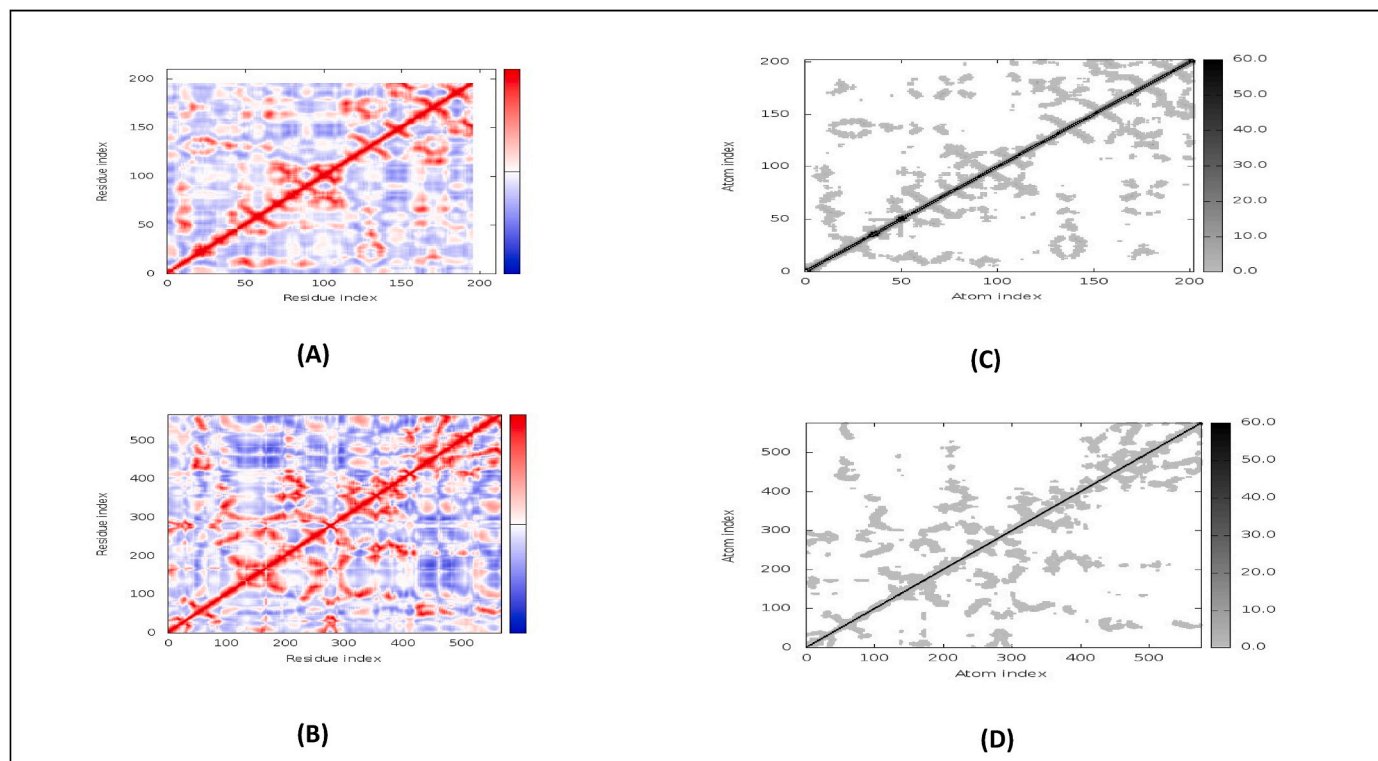


Fig. 7. Molecular dynamics simulation analysis: co-variance map: (A) Chevalone E – NS2B/NS3 protease; (B) Chevalone E – NS5 methyltransferase; and elastic network: (C) Chevalone E – NS2B/NS3 protease and (D) Chevalone E – NS5 methyltransferase.

highest solubility (Table 3). Therefore, these molecules can be used to mimic the effects of drugs (Fig. 4).

3.5. Toxicity, carcinogenicity and mutagenicity prediction

Acute toxicity, hepatotoxicity, carcinogenicity, mutagenicity, immunotoxicity, and toxicity targets were explored as the toxicity endpoints. The results revealed that Chevalone E and Brevione K fell in the category of toxicity class 4, while Sterolic acid and Brocazine A showed toxicity levels of 1 and 3, respectively (the lower the class, the higher the toxicity). The estimated LD50 for Chevalone E, Sterolic acid, Brevione K, and Brocazine A, were 1600, 34, 1255, and 75 mg/kg, respectively. The toxicity characteristics in (Table 4) depict the level of confidence in the positive toxicity results compared to the class average. No unfavorable effects such as tumorigenicity, mutagenicity, irritation, or reproductive consequences were observed for any of the compounds.

3.6. Prediction of drug targets, available drug molecules from DrugBank and molecular dynamics simulation

Molecular target investigations are required to uncover the phenotypical side effects or possible cross-reactivity caused by their actions. This is the first step in determining the viability of using the drug in future in vitro and in vivo experiments [37]. As a result, Fig. 5 shows the top 25 findings generated by SwissTargetPrediction [38] for Chevalone E (NS2B/NS3 and NS5 inhibitor), Sterolic acid (NS2B/NS3 inhibitor), and Brevione K (NS2B/NS3 and NS5 inhibitor). The target sites that the chemical could bind to were largely protease and enzyme (13.3%) for Sterolic acid, nuclear receptor (33.3%) for Chevalone E, and enzyme (26%) for Brevione K (Table 5).

Ligand-based virtual screening was used to predict biologically active small molecules against NS2B/NS3 protease and NS5 methyltransferase of dengue from DrugBank. Estramustine (DB01196) and Quinestrol (DB04575), both licensed medications, were similar to Chevalone E, with prediction scores of 0.818 and 0.856, respectively. Furthermore, the results revealed that cholic acid (DB02659), acitretin (DB00459), and mupirocin (DB00410) are similar to Sterolic acid; zidovudine (DB00495), imipenem (DB01598), and nadolol (DB01203) are similar to Brocazine A; and Budesonide (DB01222) and Colchicine (DB01394) are similar to Brevione K (Table 6). These findings indicate that these could be viable therapeutic candidates for DENV infection, implying that further research is needed. In addition, based on molecular dynamics modeling, the best complexes for NS5 methyltransferase-Chevalone E and NS2B/NS3 protease-Chevalone E showed satisfactory eigenvalues with structural stability. The maximal eigenvalue of the NS2B/NS3 protease-Chevalone E complex was $2.866006e-04$, compared to $7.701529e-05$ for the NS5 methyltransferase-Chevalone E complex, showing great flexibility and difficulty in deformation (Fig. 6 and Fig. 7).

4. Conclusions

Currently, there are no specific treatments for dengue. Although few studies have been conducted to develop dengue vaccines, this process has a great deal to be accomplished. As a result, scientists are currently looking for inhibitors to block DENV's key methyltransferase and protease, NS5 and NS2B/NS3, which are involved in viral replication, as targets for next-generation therapeutic development. On the contrary, marine fungi have proven to be a rich and promising source of novel bioactive natural compounds and may be able to suppress viral NS5 and NS2B/NS3 activities. In this study, the primary viral protease was docked against marine-derived chemicals. In addition, drug-like characteristics, toxicity, carcinogenicity, and mutagenicity were predicted using in silico ADME analysis. Analyzing the results, our study suggests that Chevalone E, Sterolic acid, Brevione K, and Brocazine A found in marine-derived fungi are the best NS5 and NS2B/NS3 inhibitors. The predicted drug based on the ligand estramustine, cholic acid, acitretin,

colchicine, and zidovudine could be exploited and developed as an alternative or complementary therapy for the treatment of dengue virus.

Funding information

This research did not receive any specific grant from funding agencies in the public, commercial, or not-for-profit sectors.

CRediT author statement

Md. Mukhtar Mia & Mahamudul Hasan: Conceptualization, Methodology, Software. Mahamudul Hasan, Shahab Uddin Munna, Md Mowdudul Hasan Talha and Kanon das: Writing- Original draft preparation. Md. Mukhtar Mia & Mahamudul Hasan: Visualization, Investigation. Md. Mukhtar Mia: Supervision. Validation. Md. Mukhtar Mia, Mahamudul Hasan, Shahab Uddin Munna, Md Mowdudul Hasan Talha: Writing- Reviewing and Editing.

Declaration of competing interest

The authors declare that they have no known competing financial interests or personal relationships that could have appeared to influence the work reported in this paper.

Acknowledgements

Authors would like to acknowledge all the members of the Faculty of Veterinary, Animal and Biomedical Sciences, (SAU) for the methodological support of the project.

Appendix A. Supplementary data

Supplementary data to this article can be found online at <https://doi.org/10.1016/j.imu.2022.100932>.

References

- [1] Dighe SN, Dua K, Chellappan DK, Katavic PL, Collet TA, others. Recent update on anti-dengue drug discovery. *Eur J Med Chem* 2019;176:431–55. <https://doi.org/10.1016/j.ejmech.2019.05.010>.
- [2] Cdc EC for DP and C. Dengue worldwide overview. <https://www.ecdc.europa.eu/en/dengue-monthly>. [Accessed 10 March 2022].
- [3] Troost B, Smit JM. Recent advances in antiviral drug development towards dengue virus. *Curr Opin Virol* 2020;43:9–21. <https://doi.org/10.1016/j.coviro.2020.07.009>.
- [4] Cabarcas-Montalvo M, Maldonado-Rojas W, Montes-Grajales D, Bertel-Sevilla A, Wagner-Doebler I, Sztajer H, et al. Discovery of antiviral molecules for dengue: in silico search and biological evaluation. *Eur J Med Chem* 2016;110:87–97. <https://doi.org/10.1016/j.ejmech.2015.12.030>.
- [5] Lou Z, Sun Y, Rao Z. Current progress in antiviral strategies. *Trends Pharmacol Sci* 2014;35:86–102. <https://doi.org/10.1016/j.tips.2013.11.006>.
- [6] Gu W, Ip DT-M, Liu S, Chan JH, Wang Y, Zhang X, et al. 1, 4-Bis (5-(naphthalen-1-yl) thiophen-2-yl) naphthalene, a small molecule, functions as a novel anti-HIV-1 inhibitor targeting the interaction between integrase and cellular Lens epithelium-derived growth factor. *Chem Biol Interact* 2014;213:21–7. <https://doi.org/10.1016/j.cbi.2014.01.011>.
- [7] Yang C-C, Hu H-S, Wu R-H, Wu S-H, Lee S-J, Jiaang W-T, et al. A novel dengue virus inhibitor, BP13944, discovered by high-throughput screening with dengue virus replicon cells selects for resistance in the viral NS2B/NS3 protease. *Antimicrob Agents Chemother* 2014;58:110–9. <https://doi.org/10.1128/AAC.01281-13>.
- [8] Rothan HA, Han HC, Ramasamy TS, Othman S, Abd Rahman N, Yusof R. Inhibition of dengue NS2B-NS3 protease and viral replication in Vero cells by recombinant retrocyclin-1. *BMC Infect Dis* 2012;12:1–9. <https://doi.org/10.1186/1471-2334-12-314>.
- [9] Hughes PJ, Cretton-Scott E, Teague A, Wensel TM. Protease inhibitors for patients with HIV-1 infection: a comparative overview. *Pharmacol Ther* 2011;36:332.
- [10] Forns X, Lawitz E, Zeuzem S, Gane E, Bronowicki JP, Andreone P, et al. Simeprevir with peginterferon and ribavirin leads to high rates of SVR in patients with HCV genotype 1 who relapsed after previous therapy: a phase 3 trial. *Gastroenterology* 2014;146:1669–79. <https://doi.org/10.1053/j.gastro.2014.02.051>.
- [11] Keating GM, Vaidya A. Sofosbuvir: first global approval. *Drugs* 2014;74:273–82. <https://doi.org/10.1007/s40265-014-0179-7>.
- [12] Yasuhara-Bell J, Lu Y. Marine compounds and their antiviral activities. *Antivir Res* 2010;86:231–40. <https://doi.org/10.1016/j.antiviral.2010.03.009>.

- [13] Dundas J, Ouyang Z, Tseng J, Binkowski A, Turpaz Y, Liang J. CASTp: computed atlas of surface topography of proteins with structural and topographical mapping of functionally annotated residues. *Nucleic Acids Res* 2006;34:W116–8. <https://doi.org/10.1093/nar/gkl282>.
- [14] Wang Y-T, Xue Y-R, Liu C-H. A brief review of bioactive metabolites derived from deep-sea fungi. *Mar Drugs* 2015;13:4594–616. <https://doi.org/10.3390/md13084594>.
- [15] Arifeen MZU, Xue Y-R, Liu C-H. Deep-sea fungi: diversity, enzymes, and bioactive metabolites. *Fungi Extrem Environ Ecol Role Biotechnol Sign* 2019;331. https://doi.org/10.1007/978-3-030-19030-9_17.
- [16] Filimonov DA, Lagunin AA, Glorizova TA, Rudik AV, Druzhilovskii DS, Pogodin PV, et al. Prediction of the biological activity spectra of organic compounds using the PASS online web resource. *Chem Heterocycl Compd* 2014;50:444–57. <https://doi.org/10.1007/s10593-014-1496-1>.
- [17] Trott O, Olson AJ. AutoDock Vina: improving the speed and accuracy of docking with a new scoring function, efficient optimization, and multithreading. *J Comput Chem* 2010;31:455–61. <https://doi.org/10.1002/jcc.21334>.
- [18] Balani SK, Miwa GT, Gan L-S, Wu J-T, Lee FW. Strategy of utilizing in vitro and in vivo ADME tools for lead optimization and drug candidate selection. *Curr Top Med Chem* 2005;5:1033–8. <https://doi.org/10.2174/156802605774297038>.
- [19] Daina A, Michielin O, Zoete V. SwissADME: a free web tool to evaluate pharmacokinetics, drug-likeness and medicinal chemistry friendliness of small molecules. *Sci Rep* 2017;7:1–13. <https://doi.org/10.1038/srep42717>.
- [20] Daina A, Zoete V. A boiled-egg to predict gastrointestinal absorption and brain penetration of small molecules. *ChemMedChem* 2016;11:1117. <https://doi.org/10.1002/cmdc.201600182>.
- [21] Pires DEV, Blundell TL, Ascher DB. pkCSM: predicting small-molecule pharmacokinetic and toxicity properties using graph-based signatures. *J Med Chem* 2015;58:4066–72. <https://doi.org/10.1021/acs.jmedchem.5b00104>.
- [22] Banerjee P, Eckert AO, Schrey AK, Preissner R. ProTox-II: a webserver for the prediction of toxicity of chemicals. *Nucleic Acids Res* 2018;46:W257–63. <https://doi.org/10.1093/nar/gky318>.
- [23] Azim KF, Ahmed SR, Banik A, Khan MMR, Deb A, Somana SR. Screening and druggability analysis of some plant metabolites against SARS-CoV-2: an integrative computational approach. *Inform Med Unlocked* 2020;20:100367. <https://doi.org/10.1016/j.imu.2020.100367>.
- [24] Drwal MN, Banerjee P, Dunkel M, Wettig MR, Preissner R. ProTox: a web server for the in silico prediction of rodent oral toxicity. *Nucleic Acids Res* 2014;42:W53–8. <https://doi.org/10.1093/nar/gku401>.
- [25] Daina A, Michielin O, Zoete V. SwissTargetPrediction: updated data and new features for efficient prediction of protein targets of small molecules. *Nucleic Acids Res* 2019;47:W357–64. <https://doi.org/10.1093/nar/gkz382>.
- [26] Zoete V, Daina A, Bovigny C, Michielin O. SwissSimilarity: a web tool for low to ultra high throughput ligand-based virtual screening. 2016. <https://doi.org/10.1021/acs.jcim.6b00174>.
- [27] Bhattacharya M, Sharma AR, Patra P, Ghosh P, Sharma G, Patra BC, et al. A SARS-CoV-2 vaccine candidate: in-silico cloning and validation. *Inform Med Unlocked* 2020;20:100394. <https://doi.org/10.1016/j.imu.2020.100394>.
- [28] Ghosh P, Bhakta S, Bhattacharya M, Sharma AR, Sharma G, Lee S-S, et al. A novel multi-epitopic peptide vaccine candidate against *Helicobacter pylori*: in-silico identification, design, cloning and validation through molecular dynamics. *Int J Pept Res Therapeut* 2021;27:1149–66. <https://doi.org/10.1007/s10989-020-10157-w>.
- [29] López-Blanco JR, Aliaga JI, Quintana-Ort\`i ES, Chacón P. iMODS: internal coordinates normal mode analysis server. *Nucleic Acids Res* 2014;42:271–6. <https://doi.org/10.1093/nar/gku339>.
- [30] Abdelli I, Hassani F, Bekkel Briki S, Ghalem S. In silico study the inhibition of angiotensin converting enzyme 2 receptor of COVID-19 by *Ammoides verticillata* components harvested from Western Algeria. *J Biomol Struct Dyn* 2020;39:1–14. <https://doi.org/10.1080/07391102.2020.1763199>.
- [31] Simon L, Imane A, Srinivasan KK, Pathak L, Daoud I. In silico drug-designing studies on flavanoids as anticancer agents: pharmacophore mapping, molecular docking, and Monte Carlo method-based QSAR modeling. *Interdiscipl Sci Comput Life Sci* 2017;9:445–58. <https://doi.org/10.1007/s12539-016-0169-4>.
- [32] Xu J, Gao L, Liang H, Chen S. In silico screening of potential anti-COVID-19 bioactive natural constituents from food sources by molecular docking. *Nutrition* 2021;82:111049. <https://doi.org/10.1016/j.nut.2020.111049>.
- [33] Rosmalena R, Elya B, Dewi BE, Fithriyah F, Desti H, Angelina M, et al. The antiviral effect of Indonesian medicinal plant extracts against dengue virus in vitro and in silico. *Pathogens* 2019;8:85. <https://doi.org/10.3390/pathogens8020085>.
- [34] Ghosh I, Talukdar P. Molecular docking and pharmacokinetics study for selected leaf phytochemicals from *Carica papaya* Linn. against dengue virus protein, NS2B/NS3 protease. *World Sci News* 2019;124:264–78.
- [35] Vora J, Patel S, Athar M, Sinha S, Chhabria MT, Jha PC, et al. Pharmacophore modeling, molecular docking and molecular dynamics simulation for screening and identifying anti-dengue phytochemicals. *J Biomol Struct Dyn* 2019. <https://doi.org/10.1080/07391102.2019.1615002>.
- [36] Lipinski CA, Lombardo F, Dominy BW, Feeney PJ. Experimental and computational approaches to estimate solubility and permeability in drug discovery and development settings. *Adv Drug Deliv Rev* 1997;23:3–25. [https://doi.org/10.1016/S0169-409X\(96\)00423-1](https://doi.org/10.1016/S0169-409X(96)00423-1).
- [37] Lucio FNM, da Silva JE, Marinho EM, Mendes FRDS, Marinho MM, Marinho ES. Methylcytosine alcaoloid potentially active against dengue virus: a molecular docking study and electronic structural characterization. *Int J Res* 2020;8:221–36.
- [38] Gfeller D, Grosdidier A, Wirth M, Daina A, Michielin O, Zoete V. SwissTargetPrediction: a web server for target prediction of bioactive small molecules. *Nucleic Acids Res* 2014;42:32–8. <https://doi.org/10.1093/nar/gku293>.
- [39] Meng L-H, Li X-M, Lv C-T, Huang C-G, Wang C-G. Brocacins A–F, cytotoxic bishiodiketopiperazine derivatives from *Penicillium brocae* MA-231, an endophytic fungus derived from the marine mangrove plant *Avicennia marina*. *J Nat Prod* 2014;77:1921–7. <https://doi.org/10.1021/np500382k>.
- [40] Prompanya C, Dethoup T, Bessa LJ, Pinto MMM, Gales L, Costa PM, et al. New isocoumarin derivatives and meroterpenoids from the marine sponge-associated fungus *Aspergillus similanensis* sp. nov. KUFA 0013. *Mar Drugs* 2014;12:5160–73. <https://doi.org/10.3390/md12105160>.
- [41] Sun Y-L, Zhang X-Y, Nong X-H, Xu X-Y, Qi S-H. New antifouling macrodiolides from the deep-sea-derived fungus *Trichobotrys effuse* DFFSCS021. *Tetrahedron Lett* 2016;57:366–70. <https://doi.org/10.1016/j.tetlet.2015.12.026>.
- [42] Yao Q, Wang J, Zhang X, Nong X, Xu X, Qi S. Cytotoxic polyketides from the deep-sea-derived fungus *Engyodontium album* DFFSCS021. *Mar Drugs* 2014;12:5902–15. <https://doi.org/10.3390/md12125902>.
- [43] Trisuwan K, Rukachaisirikul V, Kaewpet M, Phongpaichit S, Hutadilok-Towatana N, Preedanon S, et al. Sesquiterpene and xanthone derivatives from the sea fan-derived fungus *Aspergillus sydowii* PSU-F154. *J Nat Prod* 2011;74:1663–7. <https://doi.org/10.1021/np200374j> PMID:21718031.
- [44] Feng J-M, Li M, Zhao J-L, Jia X-N, Liu J-M, Zhang M, et al. Three new phenylspirodrimane derivatives with inhibitory effect towards potassium channel Kv1.3 from the fungus *Stachybotrys chartarum*. *J Asian Nat Prod Res* 2019. <https://doi.org/10.1080/10286020.2018.1551372>.
- [45] Xu Y, Espinosa-Artiles P, Schubert V, Xu Y, Zhang W, Lin M, et al. Characterization of the biosynthetic genes for 10, 11-dehydrocurvularin, a heat shock response-modulating anticancer fungal polyketide from *Aspergillus terreus*. *Appl Environ Microbiol* 2013;79:2038–47. <https://doi.org/10.1128/AEM.03334-12>.
- [46] Liu Z, Xia G, Chen S, Liu Y, Li H, She Z. Eurothiocin A and B, sulfur-containing benzofurans from a soft coral-derived fungus *Eurotium rubrum* SH-823. *Mar Drugs* 2014;12:3669–80. <https://doi.org/10.3390/md12063669>.
- [47] Spence JTJ, George JH. Biomimetic total synthesis of ent-penicillactone A and penicillactone B. *Org Lett* 2013;15:3891–3.
- [48] Li Y, Ye D, Shao Z, Cui C, Che Y. A sterol and spiroditerpenoids from a *Penicillium* sp. isolated from a deep sea sediment sample. *Mar Drugs* 2012;10:497–508. <https://doi.org/10.3390/md10020497>.
- [49] Li Y, Ye D, Chen X, Lu X, Shao Z, Zhang H, et al. Breviane spiroditerpenoids from an extreme-tolerant *Penicillium* sp. isolated from a deep sea sediment sample. *J Nat Prod* 2009;72:912–6. <https://doi.org/10.1021/np900116m>.
- [50] Li C-S, Li X-M, Gao S-S, Lu Y-H, Wang B-G. Cytotoxic anthranilic acid derivatives from deep sea sediment-derived fungus *Penicillium paneum* SD-44. *Mar Drugs* 2013;11:3068–76. <https://doi.org/10.3390/md11083068>.
- [51] Ma Y, Li J, Huang M, Liu L, Wang J, Lin Y. Six new polyketide decalin compounds from mangrove endophytic fungus *Penicillium aurantiogriseum* 328. *Mar Drugs* 2015;13:6306–18. <https://doi.org/10.3390/md13106306>.
- [52] Nakazawa T, Ishiuchi K, Sato M, Tsunematsu Y, Sugimoto S, Gotanda Y, et al. Targeted disruption of transcriptional regulators in *Chaetomium globosum* activates biosynthetic pathways and reveals transcriptional regulator-like behavior of aureoninol. *J Am Chem Soc* 2013;135:13446–55. <https://doi.org/10.1021/ja405128k>.
- [53] Fang S-M, Wu C-J, Li C-W, Cui C-B. A practical strategy to discover new antitumor compounds by activating silent metabolite production in fungi by diethyl sulphate mutagenesis. *Mar Drugs* 2014;12:1788–814. <https://doi.org/10.3390/md12041788>.
- [54] Tziveleka L-A, Vagias C, Roussis V. Natural products with anti-HIV activity from marine organisms. *Curr Top Med Chem* 2003;3:1512–35. <https://doi.org/10.2174/1568026033451790>.
- [55] Gao H, Guo W, Wang Q, Zhang L, Zhu M, Zhu T, et al. Aspulvinones from a mangrove rhizosphere soil-derived fungus *Aspergillus terreus* Gwq-48 with anti-influenza A viral (H1N1) activity. *Bioorg Med Chem Lett* 2013;23:1776–8. <https://doi.org/10.1016/j.bmcl.2013.01.051>.
- [56] Wang H, Wang Y, Wang W, Fu P, Liu P, Zhu W. Anti-influenza virus polyketides from the acid-tolerant fungus *Penicillium purpurogenum* JS03-21. *J Nat Prod* 2011;74:2014–8.
- [57] Ishii T, Hida T, Ishimaru T, Iinuma S, Sudo K, Muroi M, et al. TAN-931, A novel nonsteroidal aromatase inhibitor produced BY *Penicillium funiculosum* No. 8974. *J Antibiot (Tokyo)* 1991;44:589–99. <https://doi.org/10.7164/antibiotics.44.600> PMID: 2071487.
- [58] Peng J, Zhang X, Du L, Wang W, Zhu T, Gu Q, et al. Sorbicatechols A and B, antiviral sorbicillinoids from the marine-derived fungus *Penicillium chrysogenum* PJX-17. *J Nat Prod* 2014;77:424–8. <https://doi.org/10.1021/np400977e> PMID: 24495078.
- [59] Zheng C-J, Shao C-L, Guo Z-Y, Chen J-F, Deng D-S, Yang K-L, et al. Bioactive hydroanthraquinones and anthraquinone dimers from a soft coral-derived *Alternaria* sp. fungus. *J Nat Prod* 2012;75:189–97. <https://doi.org/10.1021/np200766d> PMID:22276679.
- [60] Cheng Z, Zhao J, Liu D, Proksch P, Zhao Z, Lin W. Eremophilane-type sesquiterpenoids from an *acremonium* sp. fungus isolated from deep-sea sediments. *J Nat Prod* 2016;79:1035–47. <https://doi.org/10.1021/acs.jnatprod.5b01103> PMID:26928174.
- [61] Wang J-F, Zhou L-M, Chen S-T, Yang B, Liao S-R, Kong F-D, et al. New chlorinated diphenyl ethers and xanthenes from a deep-sea-derived fungus *Penicillium chrysogenum* SCSIO 41001. *Fitoterapia* 2018;125:49–54. <https://doi.org/10.1016/j.fitote.2017.12.012>.

- [62] Wu B, Wiese J, Labes A, Kramer A, Schmaljohann R, Imhoff JF. Lindgomycin, an unusual antibiotic polyketide from a marine fungus of the Lindgomycetaceae. *Mar Drugs* 2015;13:4617–32. <https://doi.org/10.3390/md13084617>.
- [63] Lan W-J, Liu W, Liang W-L, Xu Z, Le X, Xu J, et al. Pseudaboydins A and B: novel isobenzofuranone derivatives from marine fungus *Pseudallescheria boydii* associated with starfish *Acanthaster planci*. *Mar Drugs* 2014;12:4188–99. <https://doi.org/10.3390/md12074188>.
- [64] Liu Y, Zhao S, Ding W, Wang P, Yang X, Xu J. Methylthio-aspothalasins from a marine-derived fungus *Aspergillus* sp. *Mar Drugs* 2014;12:5124–31. <https://doi.org/10.3390/md12105124>.
- [65] Kong F, Wang Y, Liu P, Dong T, Zhu W. Thiodiketopiperazines from the marine-derived fungus *Phoma* sp. OUCMDZ-1847. *J Nat Prod* 2014;77:132–7. <https://doi.org/10.1021/np400802d>.
- [66] Luo H, Li X-M, Li C-S, Wang B-G. Diphenyl ether and benzophenone derivatives from the marine mangrove-derived fungus *Penicillium* sp. MA-37. *Phytochem Lett* 2014;9:22–5. <https://doi.org/10.1016/j.phytol.2014.03.012>.
- [67] Wang J, Cox DG, Ding W, Huang G, Lin Y, Li C. Three new resveratrol derivatives from the mangrove endophytic fungus *Alternaria* sp. *Mar Drugs* 2014;12:2840–50. <https://doi.org/10.3390/md12052840>.
- [68] Hu X, Xia Q-W, Zhao Y-Y, Zheng Q-H, Liu Q-Y, Chen L, et al. Speradines F–H, three new oxindole alkaloids from the marine-derived fungus *Aspergillus oryzae*. *Chem Pharm Bull* 2014;c14–00312. <https://doi.org/10.1248/cpb.c14-00312>.